Chapter 1
Introduction

This first chapter provides an introduction to the basic principles of optoelectronics, which will be useful for the design and operational understanding of the optoelectronic device and material combinations presented in this book. It starts with a description of the general properties of organic semiconductors. We focus on the principle of conjugation and briefly discuss transport in disordered organic semiconductors. Attention is also given to the different radiative and nonradiative transitions possible in organic compounds. Organic light-emitting diodes and organic light-emitting transistors are the subject of the second section. The working principle of both devices is discussed and contrasted. Section 1.3 then focuses on another optoelectronic device, the organic semiconductor laser. First, general aspects of laser activity and the motivation for plastic lasers are considered. Next, lasing in organic semiconductors and the difficulties in achieving electrical pumping are discussed. As a conclusion to this introduction, Sect. 1.4 gives an outline of the subsequent chapters of this book.

1.1 Organic Semiconductors

In general, organic materials are compounds with a sequence of carbon atoms as backbone. Originally these carbon-based materials were considered as being insulating. In the 1950s, photoconductivity was reported for the first time in organic crystals such as anthracene and naphthalene [1–3]. The main breakthrough for organic electronics, however, took place in 1977 when Shirakawa, MacDiarmid and Heeger demonstrated that the conductivity of conjugated polymers could be varied over the full range from insulator to metal by chemical doping [4]. Since then, remarkable progress has been made in synthesizing conjugated polymers and organic small molecules, in understanding their properties, and in developing them for use in electronic and optical devices.

S. Schols, *Device Architecture and Materials for Organic Light-Emitting Devices*,
DOI 10.1007/978-94-007-1608-7_1,

1.1.1 Semiconducting Properties of Organic Materials

The semiconducting characteristics of several organic materials are the result of the properties of the atomic carbon atom. The electronic configuration of the ground state of a carbon atom is $1s^2 2s^2 2p^2$. In this configuration only the two unpaired p electrons in the outer electronic shell are able to form a bond with another atom, leading to e.g. the formation of methylene (CH_2). Mostly, however, the bonding is described by hybridization. Hybridization of the different atomic orbitals leads to more stable molecules and makes it possible to obtain a new set of hybrid orbitals, having an orientation in space matching the actual geometry of the compound much better [5]. Different hybridizations are possible: sp^3, sp^2 and sp hybridization (Fig. 1.1).

For organic semiconducting materials, the sp^2 hybridization is the most important one. In this case, the 2s orbital and two of the three 2p orbitals will combine to form three sp^2 hybrid orbitals. These three sp^2 hybrid orbitals are coplanar, having an angle of 120° between them (Fig. 1.1(b)), and will form three covalent σ-bonds with neighboring atoms, which are strongly localized in molecular σ-orbitals. The remaining 2p orbital, which is not used during hybridization, is positioned perpendicular to this plane. If two unhybridized 2p orbitals of neighboring atoms overlap, an additional π-bond is formed via π-orbitals. The overlap region and thus the electron density of this π-bond is located above and below the plane of the σ-bonds. The combination of a sp^2-sp^2 σ-bond and a 2p-2p π-bond between two neighboring carbon atoms is referred to as a double bond (C=C). If the number of sp^2 hybridized carbon atoms is increased, a conjugated system with alternating single and double bonds is formed. The simplest example of such a system is polyacetylene. In conjugated systems, the π-orbitals ideally extend over the complete molecule (the π-molecular orbital) and a delocalized electron cloud is created. The delocalized electrons are shared by all atoms of the conjugated molecule and can move freely over the entire molecule.

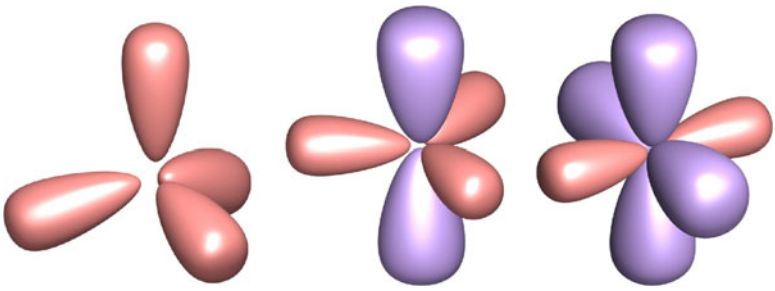

(a) sp^3 hybridization (b) sp^2 hybridization (c) sp hybridization

Fig. 1.1 Different hybridizations for the carbon atom. Sp^3 hybridization has a tetrahedral oriented structure, sp^2 hybridization forms a trigonal-planar geometry and the two sp hybrid orbitals are oriented along the same axis

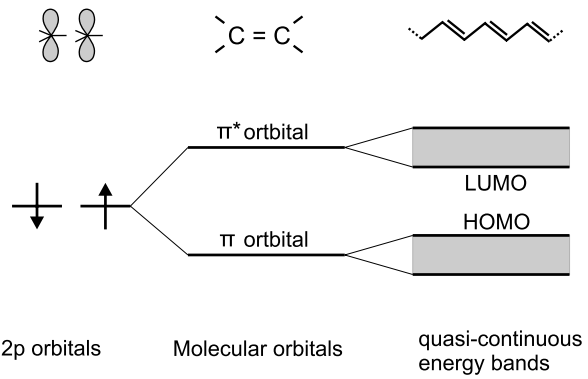

Fig. 1.2 Schematical representation of the splitting of two 2p orbitals into a bonding molecular π-orbital and an anti-bonding molecular π^*-orbital. Increasing the number of carbon atoms, leads to more degeneration and the formation of quasi-continuous bands of occupied and unoccupied states

In general, overlap and (linear) combination of orbitals give rise to the formation of new, more extended orbitals. This process is denoted by the term 'splitting'. The energy of these new orbitals with respect to each other and the original orbitals depends on the energy and overlap of the original orbitals: the stronger the overlap, the larger the splitting. In Fig. 1.2 we combine the 2p orbitals of two carbon atoms to a bonding molecular π-orbital and an anti-bonding molecular π^*-orbital. As can be seen from Fig. 1.2 the bonding molecular π-orbital and the anti-bonding molecular π^*-orbital are, respectively, lower and higher in energy than the original atomic orbitals. Every 2p orbital has only one electron and therefore, according to the Pauli principle, only the bonding molecular π-orbital will be occupied in the ground state. The anti-bonding π^*-orbital is unoccupied. When more atoms are added, more bonding and anti-bonding orbitals with different energies are created. Clearly, if the number of carbon atoms goes to infinity, the π and π^* energy levels will form quasi-continuous bands. The highest molecular orbital that still contains electrons at 0 K is called the highest occupied molecular orbital (HOMO). The lowest molecular orbital that has no electrons at 0 K is referred to as the lowest unoccupied molecular orbital (LUMO). Typically, the HOMO and LUMO are separated by an energy gap, which induces semiconducting properties in these materials. The larger the molecule, the broader the energy bands and thus the smaller the band gap will be. In general, the energy gap in organic semiconducting materials is relatively large (2 to 5 eV) compared to inorganic semiconductors (1.1 eV for silicon and 1.4 eV for GaAs [6]).

Usually, in organic electronics thin solid films are studied rather than single organic molecules. Similar to the molecular level, molecular orbitals of neighboring conjugated molecules will interact and overlap. According to molecular orbital theory these molecular orbitals will split again and form intermolecular orbitals. The intermolecular overlap, however, is typically much smaller than the intramolecular overlap because of the larger distances and weaker interactions between molecules than those between atoms. Therefore, splitting and intermolecular delocalization are significantly smaller and electrons will have much less tendency to be delocalized over the complete film. As a consequence, charge transport is not limited by the transport within one molecule, but rather by the transport from one molecule to

another. This clearly indicates that in order to obtain efficient charge transport the intermolecular overlap has to be optimized.

So far, the energy states were assumed to be located in a neutral crystal without excess charge. However, when an excess charge is placed on a molecule, an electric field is created, polarizing the environment in order to stabilize the excess charge. As a consequence, the molecule and its nearest neighbor environment relax their structure to obtain a new equilibrium. Different polarization effects can take place at different time scales: electronic polarization, molecular polarization and lattice polarization [7]. These polarization effects significantly lower the energy gap [7] and strongly influence charge transport. The charge together with its accompanying polarization forms a quasi-particle that is referred to as a polaron. Generally, hopping transport is seen for organic materials, where polarons jump from one molecule to the next [8]. The structural relaxation during polaron formation also results in the creation of two new energy levels within the band gap, allowing new electronic transitions (e.g. polaron absorption).

1.1.2 Charge Transport in Organic Materials

Similar to inorganic semiconductors, charge transport in organic materials occurs via drift and diffusion. The exact transport mechanism, however, is much more complicated due to the more complex, molecular nature of organic materials. As mentioned before, charge transport through the material is impeded due to polarization effects and due to the larger intermolecular distances and smaller intermolecular orbital overlap compared to inorganic semiconductors. Several theories have been proposed to describe charge transport in organic semiconducting materials, however, none of them can explain all experimental observations. Probably, several mechanisms occur at the same time and depending on the specific conditions charge transport is dominated by one of these mechanisms. In this section a very brief overview of the models that are often used to explain charge transport in organic semiconductors is given. For a more complete overview of relevant charge transport theories we refer to literature [7, 9, 10].

Band Transport Model

In the band model intermolecular interactions lead to the formation of energy bands in which electrons and holes can be transported freely. Band transport thus occurs in delocalized states and is limited by scattering of lattice vibrations. Since these lattice vibrations are reduced at low temperatures, the band transport model suggests that the charge carrier mobility increases with decreasing temperature. Typically, band transport is observed in inorganic semiconductors, which are highly ordered with strong coupling between the atoms. Most organic semiconductors, however, are characterized by a high degree of disorder and the weak electronic coupling (Van

der Waals and dipole-dipole interactions) between different molecules can easily be broken, causing localized instead of delocalized states. Consequently, band transport is generally not the transport mechanism in organic semiconductors. Only for highly ordered molecular crystals such as naphtalene [11], anthracene [12], rubrene [13] and pentacene [14], this behavior, indicated by an increase of the mobility at lower temperatures, has been observed.

Multiple Trapping and Release Model

The multiple trapping and release model (MTR) is originally developed to describe charge transport in hydrogenated amorphous silicon [15], but it is sometimes used to explain transport in disordered organic materials [16]. The model assumes that charge transport occurs through delocalized, extended states. Transport is, however, impeded by impurities, defects, grain boundaries, etc., which create a distribution of traps near the transport band. During charge transport charge carriers can be trapped. These trapped carriers can then, after a certain time, be thermally released to reach the transport band, where they can be trapped again. The time the carriers are trapped depends strongly on the temperature and on the depth of the trap. The higher the temperature and the shallower the trap, the faster the carriers are released. The MTR model predicts an Arrhenius-like temperature dependence of the mobility [15]. In organic semiconductor films the distribution of energy levels below the nominal LUMO or HOMO is to a large extent due to disorder. The MTR model has been used quite successfully to describe transport in these films [16, 17], despite the fact that the—more complex—hopping model, described below, is physically more relevant.

Hopping Transport Model

Because of the weak intermolecular coupling in disordered organic semiconductors, the states for charge carriers in these material systems are considered as localized instead of delocalized. Charge carrier transport is then typically described by hopping [18, 19], i.e., thermally activated tunneling of carriers between localized states. In the hopping transport model, the mobility of the charge carriers depends on their energy within the density of states distribution and increases if the density of neighboring states (in space) is large, and/or if there are states available at lower energy [7]. As mentioned before, charge transport in organic disordered semiconductors is mainly influenced by polarization effects. Polarization acts as a potential well, impeding the movements of the charge. Hopping can then be seen as polarons jumping from one site to the next. At elevated temperatures, thermal energy is sufficient to overcome small energy barriers. At low temperature, however, transport only takes place via tunneling. In general, charge transport in disordered organic semiconductors is described as a series of carrier hops from one site to the next, followed by polaronic relaxation.

1.1.3 Optical Transitions in Organic Materials

A molecular system typically consists of various energy levels. These energy levels are mainly electronic, but also vibrational, rotational and translational levels exist. Upon optical excitation of a molecule in the UV/VIS spectral range an electron can be promoted from the HOMO to the LUMO or to a higher located empty orbital. Similar to the presence of excess charges, an electric field is created and the surrounding molecules are polarized. The quasi-particle of an excited molecule that is formed in this way is an excitonic polaron, but more often the term 'exciton' is used.

The different energy levels of a molecule and the transitions between them can be described by a Jablonski diagram [20], as shown in Fig. 1.3. In this diagram the states are arranged vertically by energy and grouped horizontally by spin multiplicity. A distinction is made between singlet excitons and triplet excitons. A singlet exciton is characterized by the presence of two unpaired electrons with opposite spin (total spin-momentum is equal to 0), whereas a triplet exciton comprises two unpaired electrons with equal spin (total spin-momentum equals 1). Because of the repulsive nature of the spin-spin interactions between electrons of the same spin, a triplet state has a lower energy than the corresponding singlet state. In the diagram the singlet and triplet states are arranged and numbered in order of increasing energy (S_i and T_i). S_0 represents the ground state, which is intrinsically a singlet state in almost all organic compounds. Each electronic level possesses a vibrational manifold with typical sublevel spacing on the order of $\sim$0.1 eV. Each vibronic sublevel corresponds for his part to a manifold of rotational and translational levels with $\sim$0.01 eV internal spacing. In general, radiative transitions are indicated by straight arrows and nonradiative transitions by squiggly arrows. The vibrational ground states of each electronic state are indicated with thick lines, the higher vibrational states with thinner lines.

Absorption of a photon can promote an electron from the ground state to an excited state. Such an excited state can release its excess energy via different mechanisms. A first way is by the emission of a photon, which is called fluorescence or phosphorescence depending on the multiplicity of the excited state. Fluorescence is a rapid radiative process in which the spin multiplicities of the initial and the final states are the same. Phosphorescence, on the other hand, involves the transition from the T_1 excited state to the S_0 ground state, requiring spin-orbit coupling to conserve total momentum. Because this transition is spin-forbidden, its intensity is orders of magnitude smaller than the intensity of fluorescence from singlet excited states. For the same reason the lifetime of the triplet state is very long, up to ms or even sec, compared to ns for fluorescence [20]. During this long lifetime of the triplet state, the exciton is liable to diffusion towards trap states or to bimolecular reactions with other excitations such as triplet excitons, singlet excitons or charge carriers. These competing processes often prevent the observation of phosphorescence, especially at room temperature. Apart from radiative transitions, the excited state can also release its excess energy via nonradiative processes. Relaxation of the excited state to its lowest vibrational level is called vibronic relaxation (VR). This

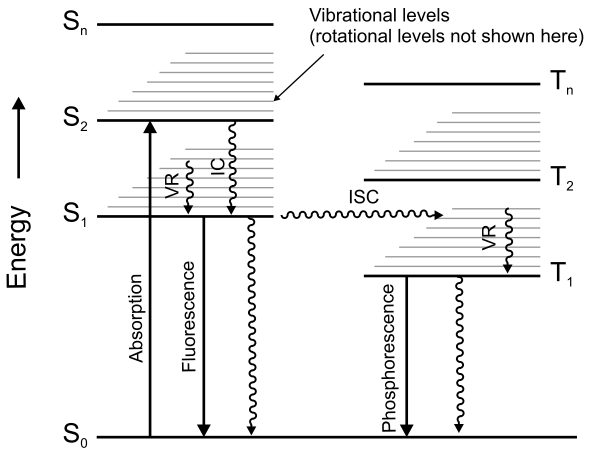

Fig. 1.3 Jablonski diagram illustrating the different energy levels of an organic molecule and indicating the possible transitions between them

process involves the dissipation of energy from the molecule to its surrounding environment and is very fast ($<10^{-12}$ s) [21]. VR is enhanced by physical contact of an excited molecule with other particles with which energy, in the form of vibrations and rotations, can be transferred through collisions. A second type of nonradiative transitions is internal conversion (IC), which occurs when a vibrational state of an electronically excited state couples to an isoenergetic vibrational state of a lower electronic state with the same spin multiplicity. IC between higher excited states ($S_n \rightarrow S_m$ and $T_n \rightarrow T_m$) occurs on the sub ps-timescale [22]. On the other hand, IC from the first excited singlet state S_1 is much slower, making fluorescence possible. A third type is intersystem crossing (ISC); this is a radiationless transition to a state with a different spin multiplicity. In molecules with large spin-orbit coupling, intersystem crossing is much more important than in molecules that exhibit only small spin-orbit coupling. Usually the triplet state is populated via ISC from the optically excited singlet state.

A very important approximation to describe the physics of an excited molecule is the Born-Oppenheimer approximation. This approximation states that the motion of the electrons can be decoupled from the motion of the nuclei because electrons have less mass and therefore respond approximately instantaneously to the movement of the nuclei. The Born-Oppenheimer approximation makes it possible to compute the wavefunction $\Psi_{molecule}$ of a molecule in two consecutive steps; it allows the wavefunction to be broken into its electronic $\Psi_{electronic}$ and nuclear (vibrational, rotational) $\Psi_{nuclear}$ components:

$$\Psi_{molecule} = \Psi_{electronic} \times \Psi_{nuclear}. \tag{1.1}$$

In other words, the energy levels of a molecule may be determined by calculating the electron energies for a fixed nuclear position. By repeating this calculation for different nuclear arrangements, the equilibrium structure of the molecule can be determined and the molecular potential energy curve as function of the configurational coordinates can be constructed (Fig. 1.4). In such a diagram an optical transition is represented by a vertical line according to the Franck-Condon principle [20]. This

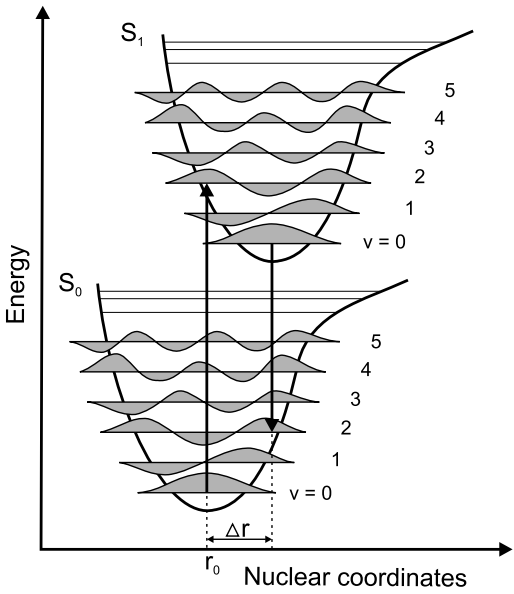

Fig. 1.4 Molecular potential energy curves for the ground state S_0 and the excited state S_1 of a diatomic molecule. According to the Franck-Condon principle, electronic transitions are very fast compared with nuclear motions and therefore vibrational levels are favored when they correspond to a minimal change in the nuclear coordinates. In this particular case transitions between $\nu = 0$ and $\nu = 2$ will be favored. r_0 is the equilibrium distance and Δr is the nuclear displacement. Absorption and emission are indicated by the vertical arrows

principle, which is the analog of the Born-Oppenheimer approximation for optical transitions, states that electronic transitions are essentially instantaneous compared with the time scale of nuclear motions. Therefore if the molecule has to move to a new vibrational level during the electronic transition, this new vibrational level must be instantaneously compatible with the nuclear position and momentum of the vibrational level of the molecule in the originating electronic state. After electronic transition the molecule will relax and obtain its equilibrium configuration. Figure 1.4 represents the potential energy curves for the ground state S_0 and the excited state S_1 of a diatomic molecule. Upon absorption of a photon of the necessary energy, an electronic transition from the $\nu = 0$ vibrational level of the ground state to the excited state occurs, indicated by a vertical line connecting the two potential energy surfaces. In the figure the situation where excitation leads to a geometrical change is illustrated. This geometrical change is indicated by a shift in nuclear coordinates between the S_0 and the S_1 state (Δr). According to the Franck-Condon principle, the probability that the molecule can end up in any particular vibrational level is proportional to the square of the (vertical) overlap of the vibrational wavefunctions of the original and final state. For this particular example, this means that the $(0 \rightarrow 2)$ vibrational transition will be the strongest. After electronic transition the molecule quickly relaxes to the lowest vibrational level, and from there it can decay to the S_0 state via photon emission. The Franck-Condon principle is applied equally to absorption and to fluorescence. As a consequence, the emission spectrum is red-shifted with respect to the absorption spectrum. This red-shift is known as the Stokes shift and varies form 0.1 eV to 1 eV in most organic compounds [21].

1.2 State of the Art Organic Light-Emitting Devices

Since the first report of electroluminescence (EL) in organic thin films [23], organic light-emitting devices have gained significant attention. In the last decade remarkable progress has been achieved in the development of organic light-emitting diodes using polymers as well as small molecule semiconductors [24]. Today, they are considered to be one of most promising technologies for display and lighting applications. Another class of organic light-emitting devices that is increasingly attracting interest is the organic light-emitting transistor. The main aspects of both device architectures will be discussed in this section.

1.2.1 Organic Light-Emitting Diodes

Although the first EL from organic materials was reported in 1953 [25, 26], it was only in 1987 that the first efficient organic light-emitting diode (OLED) comprising a bilayer heterojunction structure was demonstrated [23]. For the first time a reasonable brightness was achieved from an organic light-emitting device when a voltage below 10 V was applied. Shortly afterwards, in 1990, green-yellow EL was obtained from the conjugated polymer PPV[1] in a single layer device structure [27]. Since then, there has been an increasing research activity in the field of organic electroluminescent devices. Considerable effort has been put into the design of new materials and the improvement of color purity, luminescence efficiency and device stability [24, 28]. Today, one has succeeded in solving most critical issues and the first OLED applications are already commercially available. In the future, OLEDs may play an important role in flat panel displays and ambient lighting [29].

OLEDs are typically fabricated by sandwiching one or more appropriate organic layers between two conductive electrodes, a concept invented by S.A. VanSlyke and C.W. Tang [30]. To allow the emitted light to emerge from the device, one of the electrodes is made transparent. The conductive oxide indium tin oxide (ITO) is commonly used for this purpose. When a positive bias is applied to the ITO, electrons and holes are injected into the device and under influence of the applied electrical field these carriers travel through the organic layer or organic layers. It is shown that the current in OLEDs is typically space charge limited [9, 31], i.e., limited by the bulk of the semiconductor. In other words, the measured current is a drift current, determined by the mobility of the charge carriers. Charge transport occurs in the vertical direction, perpendicular to the stack of the organic layers, and the carrier mobility in the organic semiconductor element of OLEDs is typically low [31, 32]. When a pair of oppositely charged carriers meet, excitons are formed and radiative relaxation of these excitons results in light-emission. A schematic representation of the working principle of an OLED is illustrated in Fig. 1.5.

[1] Poly(phenylene vinylene).

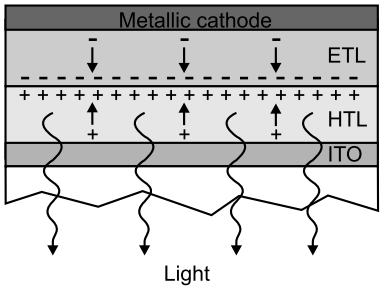

Fig. 1.5 Schematic illustration of the working principle of a basic two-layer OLED, comprising a hole-transporting layer (HTL) and an electron-transporting layer (ETL)

The simple structure, shown in Fig. 1.5 can be modified to a three-layer architecture, in which an additional luminescent layer is introduced between the hole-transporting layer (HTL) and the electron-transporting layer (ETL). The light-emitting layer can then be chosen to have a high luminescence efficiency, whereas the ETL and the HTL can be optimized for efficient charge transport. Such heterojunction concepts have been widely used in high-performance OLEDs [33, 34].

The external EL quantum efficiency η_{ext} in OLEDs is limited by the charge balance γ, the out-coupling efficiency $\eta_{coupling}$, the photoluminescent efficiency of the material ϕ_{PL} and the singlet/triplet ratio of excitons r_{st} formed by electrical injection [35]:

$$\eta_{ext} = \gamma r_{st} \phi_{PL} \eta_{coupling} = \eta_{int} \eta_{coupling}. \tag{1.2}$$

On average one singlet and three triplets are created for each four electron-hole pairs injected in the active organic semiconductor layer of an OLED [36]. However, as discussed in Sect. 1.1.3 only singlet excitons can decay efficiently and emit light. The radiative relaxation of triplets is a forbidden relaxation process and therefore triplet excitons normally do not contribute to the luminescence of OLEDs. This limits the maximum internal quantum efficiency η_{int} to only 25% when fluorescent light-emitting molecules are used. Taking into account an out-coupling efficiency of ~20%, this means that the maximum η_{ext} of a fluorescent OLED is limited to ~5%. η_{int}, however, can be increased by incorporating heavy atom organometallic compounds as guest dopants in the light-emitting layer. This increases spin-orbit coupling, and thus enhances the spin-flip process necessary for radiative decay of triplet excitations. The incorporation of platinum and iridium-containing organometallic compounds in different hosts to harvest light-emission from triplet states in OLEDs was successfully demonstrated by Baldo *et al.* in 1998 [37]. Devices based on these phosphorescent dyes represent the best performing OLEDs to date, with η_{int} approaching 100% [34] and η_{ext} between 20% and 30% [38, 39].

The quantum efficiency of OLEDs is further limited by the photoluminescent efficiency ϕ_{PL} of the organic light-emitting material (Eq. 1.2). The photoluminescent efficiency of a molecule under optical excitation is defined as the number of emitted photons per absorbed photon and is usually measured by placing the sample in an integrating sphere. Considerable effort has gone into increasing ϕ_{PL} by optimizing the chemical design of the emissive material [40] and by incorporation of the light-emitting dye in a host matrix [41]. The third limiting factor indicated by Eq. 1.2,

the charge carrier balance γ, can be improved by reducing the injection barriers at the electrode/organic interface [42] and by matching the mobility of the holes and electrons [35], whereas roughening the substrate [43] and the use of low refractive index substrates and transparent contacts [44] may increase $\eta_{coupling}$ of OLEDs.

1.2.2 Organic Light-Emitting Transistors

Complementary to the traditional vertical light-emitting diodes, light-emitting organic field-effect transistors (LEOFETs) have been proposed as lateral light-emitting devices. Because they combine the optical output of an OLED and the gate control of an organic field-effect transistor in one single device, they may become interesting structures in the field of organic displays. Displays based on LEOFETs may eliminate the difficult integration of an organic light-emitting structure and the organic driving backplane. In addition, LEOFETs can be used to study the opto-electronic performance of organic semiconductors. In contrast to OLEDs, where charge transport occurs perpendicularly to the organic layers, charge transport in LEOFETs occurs in the plane and the carriers are transported by field-effect [45]. In field-effect transistors the current flowing between the source and the drain is modulated by applying a bias to a third contact, the gate electrode. In this way, charge carriers can be accumulated or depleted in the semiconductor close to the semiconductor/insulator interface. The gate field thus provides an additional control for the amount of charges in the organic semiconductor. In addition, the accumulated charges can flood deep traps, so that the effective mobility of the remaining carriers is larger. Typically, field-effect mobility is several orders of magnitude higher than the charge carrier mobility in a conventional OLED [46].

Although the basic concept of a LEOFET dates from 1996 [47], the development of LEOFETs is still in a relatively embryonic stage. The working principle of a LEOFET is based on simultaneous injection of electrons and holes in a double layer or an ambipolar layer by adjusting the gate-source voltage and the drain-source voltage. When the biasing conditions are so that the potential at some point in the channel equals the gate potential, the accumulated charge at that point is zero and, consequently, the electron and hole accumulation layers vanish there. Exciton formation occurs near to that point and radiative relaxation of these excitons to the ground state leads to light emission. This working principle is schematically illustrated in Fig. 1.6.

The first LEOFET was demonstrated by Hepp *et al.* [48] and was based on vacuum evaporated tetracene as the organic semiconductor. Because of a large energy barrier between the electron-injecting electrode and the LUMO of tetracene, only few electrons could be injected in the organic semiconductor. In addition, electron transport is negligible in tetracene [49], resulting in exciton formation and recombination in the immediate neighborhood of the electrode. Since 2003, many other results on tetracene based LEOFETs have been reported [50–52]. Similar LEOFETs,

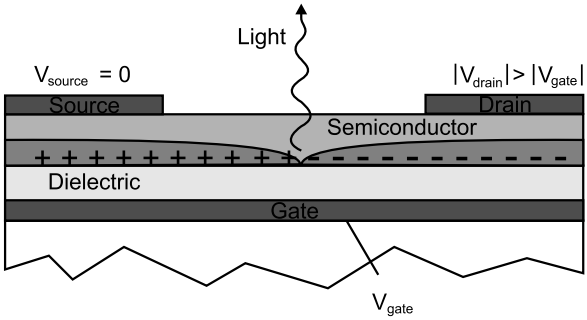

Fig. 1.6 Schematic illustration of the working principle of an ambipolar LEOFET under balanced electron and hole injection. Light-emission occurs where the electron and hole accumulation layers vanish

based on one unipolar organic semiconductor, have been realized by using polymers [53–56] as well as doped small molecules [57] as the organic semiconductor. Electroluminescence in all of these unipolar LEOFETs occurs very close to the electron-injecting metal electrode, which is one of the main drawbacks of this approach. As an alternative strategy to enhance device performance, i.e. reducing exciton quenching and light absorption at the metallic electrodes, ambipolar LEOFETs were proposed. Ambipolar LEOFETs in which the active layer is formed by a heterostructure of a p-type and an n-type organic semiconductor, either by co-evaporation [58, 59] or by subsequent evaporation of both semiconductors [60–62], were reported by different groups. Very recently, Namdas *et al.* demonstrated a solution processed bilayer LEOFET [63]. Due to the presence of an n-type and p-type organic semiconductor, electron transport occurs in a more favorable way, compared to p-type-only LEOFETs. Therefore, light-emission does not necessarily happen near the metal electrode in these devices. Another LEOFET architecture, which is also based on a heterostructure of a p-type material and en n-type material, is proposed by De Vusser *et al.* [64]. This LEOFET makes it possible to fix the location and the dimensions of the pn-junction with photolithographical resolution. In this way light-emission can be obtained inside the transistor channel, far away from the metallic electrodes. LEOFETs based on a single polymeric [65–69] or small molecule [70] ambipolar semiconductor were also reported. Zaumseil *et al.* demonstrated that the light-emission zone could be spatially controlled by varying the bias condition in such an ambipolar LEOFET [65]. Depending on the biasing conditions, the recombination zone can be moved inside the transistor channel. A near-infrared ambipolar LEOFET [71] and analytic device models for the device operation [72] and the recombination profile [73] of ambipolar LEOFETs have been proposed by Smits *et al*. More recently, light-emitting transistors based on tetracene [74], rubrene [75] and BSP-Me[2] [76] single crystal have been reported. For a detailed overview on recent progress in the field of LEOFETs, we refer to several review papers that can be found in literature [49, 77, 78].

[2] 1,4-Bis(4-methylstyryl)benzene.

1.3 Organic Semiconductor Lasers

Apart from OLEDs and LEOFETs, other optoelectronic devices have also been demonstrated in literature [79–83]. Recently, organic semiconducting materials were highlighted as a new class of solid-state laser materials [84–86]. In this section, lasing in organic semiconductors is discussed and the challenges for achieving electrically pumped lasing are put forward.

1.3.1 General Aspects of Laser Action

The first laser was demonstrated on 16 May 1960 by Theodore Maiman at Hughes Research Laboratories, by shining a high-power flash lamp on a ruby rod with silver-coated surfaces [87]. Since then, lasers have become an important instrument, not only in physical research but in almost each field of everyday life. Optical storage devices such as compact disc and DVD players are by far the largest single application of lasers, but also bar code readers, laser printers and laser pointers are well-known examples of products where laser emission is used. Other common application fields for lasers are fiber-optic communication and medicine.

The term LASER is an acronym for 'Light amplification by stimulated emission of radiation' [88] and suggests that a laser is a device emitting light through the process of stimulated emission. However, this is also true for related phenomena such as amplified spontaneous emission (ASE) or superfluorescence (SF) (Sect. 1.3.3). Therefore, seen from a laser technological point of view, a definition of the term lasing derived directly from the acronym seems insufficient. More accurately we could regard lasers as light sources that produce intense coherent light, generated by stimulated emission, and having a positive feedback mechanism [89]. Coherent light emission is the most widely known property of a laser, but since measuring first- and second order coherence of light to determine the laser threshold is impractical, alternative methods are necessary to decide whenever lasing is achieved. Generally, the following characteristics are associated with the presence of laser emission [84, 90, 91]:

- a clear indication of a threshold in the output energy as a function of the input (or pump) energy, with a high lasing efficiency above threshold
- a strong output beam polarization
- spatial coherence of the output beam
- significant spectral line narrowing (coherence in time)
- the existence of laser cavity resonances, or modes

As the acronym LASER suggests, the basic element for laser action is stimulated emission, a process first proposed by Einstein based on thermodynamic considerations. In this process the excited state is stimulated by the interaction of another photon of the same energy to relax radiatively. The crucial point about stimulated emission is the fact that the stimulated photons have the same wavelength, direction

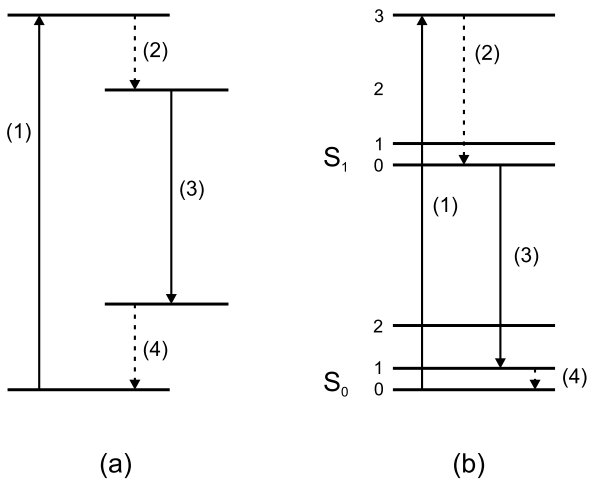

Fig. 1.7 Schematic representation of the energy levels diagrams of (**a**) a generic four-level laser material, and (**b**) the lowest two singlet states in an organic semiconductor. The transitions (*1*) and (*3*) indicate, respectively, optical absorption and emission, whereas transitions (*2*) and (*4*) are thermal relaxations

and phase as the incident ones, leading to the distinctive coherence properties of laser light. In order to achieve a significant contribution from stimulated emission, the Boltzmann equilibrium has to be disturbed in such a way that the population of the upper laser transition state exceeds the one of the lower state. This situation is known as population inversion and can be obtained in a system with more than two energy levels. In a three-level system for example, the upper laser transition state is pumped indirectly via internal conversion from a higher energy state. If the transition rate from this higher energy state to the upper laser transition state exceeds the one between the upper laser transition state and the ground state, the population can be inverted and exploited to give optical amplification by stimulated emission. A more efficient system, however, is a four-level laser system (Fig. 1.7(a)), which allows a further depopulation of the lower laser state by a fast relaxation to the ground state. This results in a higher population inversion and therefore in a more efficient stimulated amplification. The most well-known example of such a system is the He-Ne laser, but also the energy scheme of many luminescent organic materials corresponds to a four-level laser system [92]. The energy levels of a typical organic semiconductor are shown in Fig. 1.7(b). The figure shows the first excited singlet state S_1 and the ground state S_0, both split into a multitude of vibronic states. Photo-pumping from the ground state into the higher located sublevels of the excited singlet state S_1 is succeeded by a very fast non-radiative relaxation to the lowest S_1-level via vibronic relaxation. Subsequently, stimulated emission is possible from this lowest S_1-level to the vibrational states of the ground state, which are then quickly depleted via ground state relaxation.

Generally, a laser device consists of two main parts: an optical amplifier or gain medium and an optical resonator that provides the necessary optical feedback. Both parts can be recognized in Fig. 1.8, which gives a schematic representation of the most common configuration of a Fabry-Perot laser. The gain medium serves as the active material and has the properties to allow light amplification by stimulated emission. It can be of any state: gas, liquid, solid or plasma and is energetically

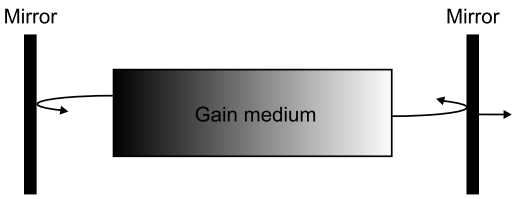

Fig. 1.8 Schematic representation of laser device structure

pumped by either optical excitation (optically pumped laser) using another laser or a flash lamp or by electrical excitation (electrical pumping). Upon excitation light is generated and photons passing through the gain medium stimulate the emission of more photons, thereby gaining in intensity when population inversion is achieved. The resonator structure then reflects the light backward and forward through the gain medium, realizing an optical oscillation. If the gain (amplification) in the medium is stronger than the resonator losses, stimulated emission can be maintained and a very intense light field is built up. The minimum pump power needed to begin laser action is called the lasing threshold. By virtue of the feedback structure building up laser oscillation is restricted to only resonant modes. Indeed, only photons aligned with the cavity manage to pass more than once through the gain medium and obtain significant amplification. The optical resonator in its most simple form consists of two end mirrors (Fig. 1.8), of which one is only partially reflective, allowing outcoupling of the output laser beam; however there are many alternative feedback designs which can be employed, such as distributed feedback (DFB) structures, micro-cavities, etc. (Sect. 1.3.3).

1.3.2 Motivation for Plastic Lasers

In the last decade, remarkable progress has been made in synthesizing organic semiconductors and in understanding their properties. Currently, organic materials have been incorporated in a number of devices, such as organic light-emitting diodes (OLEDs) [23, 27], organic photovoltaic cells [82] and organic field-effect transistors [93–95]. Notably absent from this list of electronic and optical devices, is the organic diode laser. Organic semiconductor lasers, however, possess numerous advantages over III–V semiconductor lasers, the most important being the higher integration potential on arbitrary substrates, the lower cost and the wider spectral range of possible lasing emission.

There are many photo-physical aspects that make organic semiconductors interesting materials as active laser media. The first is related to the fact that the emission spectra of organic semiconductors is broad, providing possibilities for the fabrication of tunable lasers [96–104] and broad-band optical amplification [105, 106]. In addition, the chemical structure of the organic semiconductor can be changed to give light emission across the visible spectrum. This is illustrated in Fig. 1.9, which shows the emission spectra of three common organic semiconducting laser materials. Moreover, organic materials typically have strong absorption coefficients

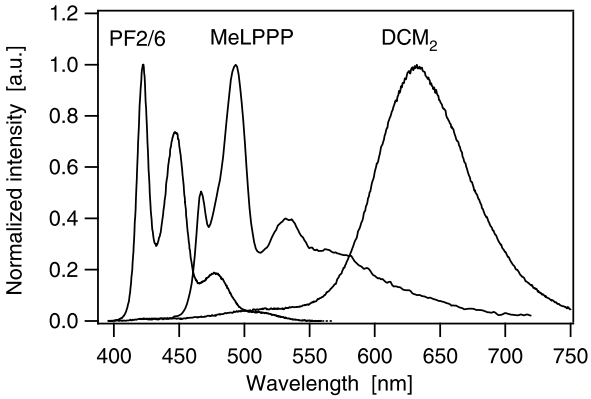

Fig. 1.9 Photoluminescence spectra of three organic semiconducting materials commonly used as laser material

($\sim 10^5$ cm^{-1}) [107], indicating that light can be absorbed over very short distances. Since stimulated emission is closely related to absorption, this means that also strong amplification is possible in organic semiconductors.

Another important property of suitable laser materials is that they have an electronic structure which corresponds to a four-level system, so that the stimulated emission spectrum does not overlap with the ground state absorption spectrum [88]. As mentioned before, most organic semiconductors naturally form a four-level system because structural and vibronic relaxation in the excited state shifts the energy levels [92]. This explains why absorption and emission spectra of organic materials are separated. Due to molecular relaxation of the excited molecules the emission spectrum is red-shifted with respect to the absorption spectrum. In organic semiconductor films, more particularly in conjugated polymer films, there is an additional factor that contributes to the separation of absorption and emission spectra. In conjugated polymers there is typically a high degree of conformational disorder, introducing a distribution of energy levels [108]. Consequently, molecules with a wide range of energies are excited, however, this energy is rapidly transferred to the lowest energy molecules, from which emission occurs [109]. This effect increases further the separation between absorption and emission and is helpful for lasing because it reduces re-absorption at the lasing wavelength.

The fact that high photoluminescence efficiencies can be obtained even in undiluted films [110–113] is another reason why organic semiconductors are attractive laser materials. Considerable effort, however, is needed to control intermolecular interactions in the solid state. The approaches to avoid quenching generally involve increasing the spacing of the chromophores (light-emitting units). For small molecules, this can be done by incorporating the light-emitting dye in a host matrix [41, 114]. In conjugated polymers, bulky side groups are often used to keep the polymer chains apart [40].

1.3.3 Lasing in Organic Semiconductors

Historical Overview of Lasing in Organic Materials

The development of organic transistors [115] and organic light-emitting diodes [23, 27] came many years after their inorganic counterparts. In contrast, organic materials have played a significant role in the development of lasers from the beginning. Lasers using organic materials were proposed in the early 1960s [116] and were demonstrated a few years later by Sorokin *et al.* using liquid solutions of organic dye molecules [117]. Due to their broad gain spectrum and wide tuning range [118] commercial dye lasers have been existing for many years and are used for various applications. However, the complex and bulky laser design, requiring regular maintenance, as well as the need to employ large volumes of organic solvents are inherent drawbacks of this technology.

The first solid-state lasers employing organic materials were demonstrated in 1967 by Soffer and McFarland using dye-doped polymers [119] and were followed by the realization of lasing in doped single crystals in 1972 [120] and in pure anthracene crystals in 1974 [121]. Since then, lasing has been demonstrated in a variety of dye-doped solid-state materials [122–125]. In all of these lasers the dye molecules were dispersed in an electrically insulating and optically transparent host matrix, taking prospects for electrical injection away due to the absence of efficient charge transport. Conjugated polymers and organic small molecules, however, may circumvent this problem. Lasing from conjugated polymers was demonstrated for the first time by Moses in 1992 employing a liquid-dye laser configuration [126]. He obtained stimulated emission from the conjugated polymer MEH-PPV[3], which was used in solution. Following this observation, stimulated emission in diluted PPVs was studied extensively and mechanisms that may obstruct lasing in neat films were discussed [127–129]. The first lasing from solid-state conjugated polymers was reported by Hide *et al.* in 1996 [130]. Similar to the solution case, the light-emitting molecules were dispersed in a polystyrene host matrix to prevent the interaction between neighboring polymer chains. Moreover, titanium dioxide (TiO_2) nanoparticles were blended into the MEH-PPV/polystyrene film to enhance scattering. Later that year, four research groups independently observed stimulated emission from neat conjugated polymer films. Graupner *et al.* observed stimulated emission from a poly(para-phenylene)-type ladder polymer using pump-probe experiments [131]. Tessler *et al.* obtained ASE by placing PPV between a dielectric and a semi-transparent silver mirror to form a microcavity [132]. Similar results were obtained by Hide *et al.* [133] and Frolov *et al.* [134] who observed line narrowing in optically pumped waveguides of PPV derivatives. These observations showed for the first time that neat films of conjugated polymers, which are capable of conducting current, could amplify light and that it was not unreasonable to attempt making polymer diode lasers. Apart from conjugated polymers, organic

[3] Poly(2-methoxy-5-(2'-ethyl-hexyloxy)-1,4-phenylene vinylene).

small molecules are also promising laser materials. Optically pumped lasers based on thin films of evaporated organic small molecules were demonstrated by Kozlov *et al.* [90] and Berggren *et al.* [135] in 1997. Since then, lasing action has been studied in different organic semiconductors [136–142] and in a variety of optically pumped structures [143–148], demonstrating the feasibility of organic thin-film materials as active laser media.

Stimulated Emission and Gain in Organic Semiconductors

A prerequisite for lasing is the presence of stimulated emission, which is quantified by the wavelength dependent cross-section for stimulated emission $\sigma_{SE}(\lambda)$. The wavelength dependence of $\sigma_{SE}(\lambda)$ typically resembles the photoluminescence spectrum of the material and is given by:

$$\sigma_{SE}(\lambda) = \frac{\lambda^4 f(\lambda)}{8\pi n^2 c \tau_r}, \tag{1.3}$$

where $f(\lambda)$ is the normalized spectral distribution of the photoluminescence, n is the refractive index of the material, c is the speed of light in free space and τ_r is the radiative lifetime of the involved optical transition. Using this relation, the cross-section for stimulated emission in organic semiconductors can be estimated. For conjugated polymers values in the range of 10^{-16} cm^2 are calculated [149]. This was experimentally confirmed by Haugeneder *et al.* [150] and Holzer *et al.* [151] who measured respectively the cross-section for stimulated emission of LPPP[4] and PmPV-co-DOctOPV[5]. The high cross-sections for stimulated emission measured in conjugated polymers is mainly due to the fact that the π–π^* transitions are fully allowed.

When population inversion is achieved and light travels through an amplifying medium its intensity I increases exponentially with the distance l traveled through the gain medium:

$$I = I_0 \exp[(g - \alpha)l], \tag{1.4}$$

where I_0 is the initial intensity, g is the gain coefficient of the material and α is the loss coefficient. Equation 1.4 clearly shows that lasing is the result of a balance between optical gain and losses in the sample. The gain coefficient is related to the density of excited states N_{exc} and $\sigma_{SE}(\lambda)$ via:

$$g(\lambda) = \sigma_{SE}(\lambda) N_{exc} \Gamma, \tag{1.5}$$

where Γ is the optical confinement factor (i.e. the fraction of the optical wave located in the active layer).

Three main factors determine the overall gain spectrum of an optically pumped organic semiconductor: the gain spectrum of the material, the ground-state absorption and the excited-state absorption. Excited-state absorption is the absorption from

[4] Ladder-type poly(para-phenylene).

[5] Poly(*m*-phenylenevinylene-*co*-2,5-dioctoxy-p-phenylenevinylene).

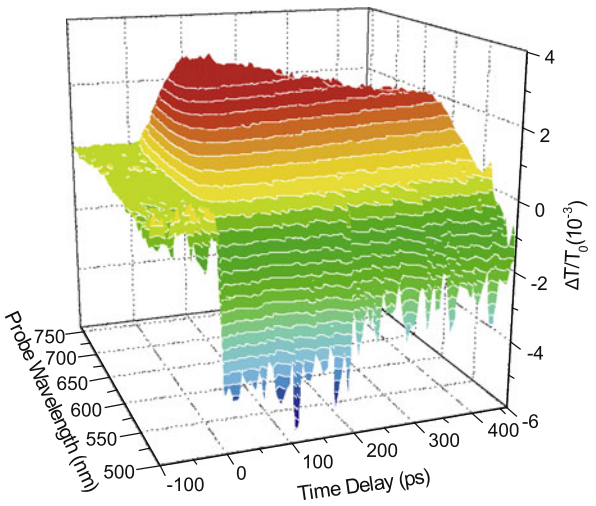

Fig. 1.10 Transient absorption measurement on a 150-nm thick layer of Alq_3 doped with 2%wt DCM_2 deposited on a quartz substrate (Measurements performed by RWTH Aachen)

the radiative S_1-state to higher located energy levels and tends to be problematic for many laser materials. Only when there is no spectral overlap between the gain spectrum of the material and the excited-state absorption, stimulated emission can be obtained. Another competing absorption process is triplet absorption, which arises from those molecules that undergo intersystem crossing and populate the triplet state. The absorption from the T_1-state to the higher located triplet states is particularly important for continuous wave operation, since in this case the population in the T_1-level may accumulate due to the much longer lifetime of the triplet state.

There have been two main approaches to study gain in potential organic semiconductor laser materials. The first is by transient absorption spectroscopy and the second is by measuring amplified spontaneous emission (ASE). Transient absorption measurements or time-resolved pump-probe measurements are a technique that allows ultra-fast measurements of photo-excitations. The sample is typically excited (pumped) by a fast femtosecond laser pulse, which generates photo-excitations, while weaker pulses of light at varying time delays and with varying wavelengths are used to probe the sample. The newly formed photo-excitations then absorb in some parts of the spectrum, while in other parts of the spectrum there is a reduction of the absorption due to the reduced population in the ground state. Therefore, at wavelengths where there is gain, the probe beam will be amplified, whereas at wavelengths where competing absorption processes are dominant, the probe beam is attenuated. An example of such a measurement is shown in Fig. 1.10. The positive transmission change between 550 nm and 730 nm is due to stimulated emission.

The first observation of stimulated emission was reported by Yan *et al.* who performed transient absorption measurements on PPV [152]. In this study, however, the gain was extremely short-lived, which was attributed to the fast formation of intermolecular photo-excitations with strong photo-induced absorption, reducing the net gain in the sample. Since then, several reports have confirmed that high gain is

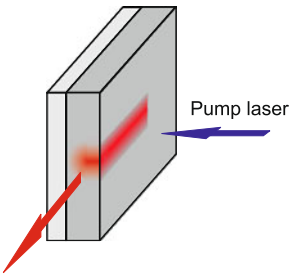

Fig. 1.11 Schematic representation of the typical experimental configuration used for ASE measurements

possible in organic semiconductors [153–156]. MeLPPP[6], for example, has a gain coefficient of around 2000 cm^{-1} [157]. These reports, however, also show that the gain lifetime is usually short, in the order of picoseconds [158]. This represents a challenge for lasers, because a short excited-state lifetime means that a high pumping rate is needed to maintain population inversion [86]. In literature different approaches are suggested to enhance stimulated emission. Denton *et al.* indicated that photo-oxidation must be avoided to obtain maximum gain [129], but also dilution of a polymer in a host matrix can be used to increase the overall gain [127]. For future electrically pumped devices, however, this latter approach might not be useful since charge transport is strongly reduced in diluted systems [159]. In addition, one should keep in mind that the photophysical properties of organic semiconductor films are quite sensitive to packing morphology, which can vary dramatically upon preparation conditions [160, 161].

Although transient absorption spectroscopy provides a powerful means for studying stimulated emission and its competing processes, it is not the easiest method to characterize an organic semiconductor as a laser material. A much easier technique to study gain in organic materials is by measuring amplified spontaneous emission (ASE). This technique involves photo-pumping a slab waveguide in a stripe near the edge of the sample and collecting the edge emission. Typically, the thin-film waveguide is made by depositing the organic semiconductor on a substrate with low refractive index. A schematic representation of the experimental configuration is shown in Fig. 1.11.

When the pump intensity is high enough for the gain to exceed the scattering losses, spontaneously emitted photons are exponentially amplified by stimulated emission according to Eq. 1.4. Since photons whose energy coincides with the spectral position of maximum gain will be amplified more than others a collapse of the emission spectrum, called gain narrowing, is observed. The change in spectral shape upon excitation density is illustrated in Fig. 1.12. This figure depicts the edge-emitted spectra of a 150-nm thick MeLPPP film on glass for two different pump powers. At a laser fluence below the ASE threshold (full line, normalized) a broad emission spectrum spanning from 450 to 700 nm is observed. This is attributed to spontaneous emission of MeLPPP molecules, which are populated in an excited state via optical pumping. Increasing the excitation fluence to higher values

[6]Methyl-substituted ladder-type poly(para-phenylene).

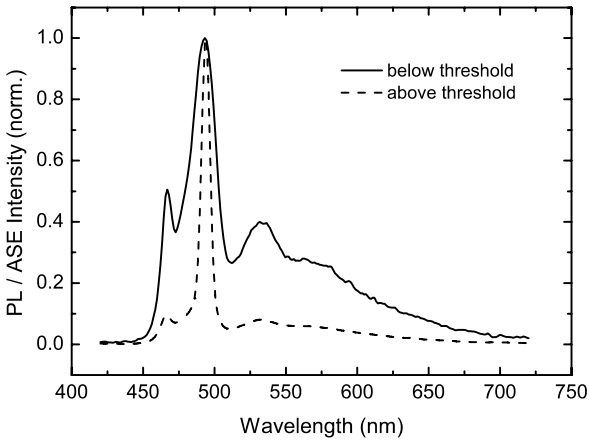

Fig. 1.12 Edge-detected emission spectra of a 150-nm thick MeLPPP film measured at different pump powers. The normalized spectra show a significant spectral gain narrowing at high excitation densities, indicating that ASE has become the dominant deactivation pathway

(dashed line, normalized) results in a spectral narrowing around the peak emission wavelength of 495 nm, which is characteristic for ASE. Here, spontaneously emitted photons, propagating across the optically pumped region, stimulate the emission of excited molecules. In literature ASE has been demonstrated using various organic semiconductors [137, 138, 162–164]. The lowest ASE threshold reported to date is obtained in films based on spiro-SBCz[7] [56].

To extract the gain coefficient from ASE measurements, the variable stripe length method can be applied [165, 166]. In this method the line-narrowed emission is measured as a function of the pump stripe length. The wavelength dependent output intensity, $I(\lambda)$, of the ASE is then given by the expression:

$$I(\lambda) = \frac{A(\lambda) I_p}{g(\lambda)} (\exp(g(\lambda) l) - 1), \tag{1.6}$$

where $A(\lambda)$ is a constant related to the cross-section for spontaneous emission, I_p is the pumping intensity, $g(\lambda)$ is the net gain coefficient, and l is the length of the pumped stripe. By fitting the experimentally measured data to Eq. 1.6 the net gain of the waveguide can be calculated. This method was developed twenty years ago for the inorganic semiconductor cadmium sulfide [165], but has since then been widely applied to determine the gain of organic semiconductors [163, 164, 167, 168]. In addition, this technique provides an easy way to distinguish between ASE and other mechanisms that were proposed to explain the observed spectral narrowing, such as superfluorescence [134, 169] or bi-excitonic emission [170]. If ASE occurs, the spectra should be broad at short stripe lengths and spectral narrowing should occur when the excitation length increases. In contrast, if superfluorescence or bi-excitonic emission is the mechanism of spectral narrowing, the emission spectrum should not depend on the size of the excitation region [85].

The net gain obtained from variable stripe length experiments is determined by waveguide losses, which can arise form self-absorption or scattering. Experiments

[7] 2,7-bis[4-(N-carbazole)phenylvinyl]-9,9'-spirobifluorene.

similar to the net gain measurements can be performed to measure these losses. The pump stripe, having a fixed length, is then progressively moved away from the edge of the sample. Since the emission from the end of the pumped region, I_0, is constant, the emission from the edge of the sample decreases according to Eq. 1.4. Waveguide losses in conjugated polymers typically lie in the range of 3–50 cm^{-1} [86], although even lower losses (<1 cm^{-1}) have been reported in blended organic thin films using cascade energy transfer [135].

Feedback Structures for Organic Semiconductor Lasers

Although ASE has many properties of lasing, such as a distinct threshold and the emission of concentrated, polarized and almost monochromatic light, the above described structures are no lasers because of the absence of resonant modes. Consequently, the output beam obtained in ASE experiments is incoherent. In order to obtain coherent light emission, the gain medium should be incorporated into a resonator, which provides optical feedback. The most common approach to make a resonator is by placing the gain medium between two mirrors. Light is then reflected back and forth between these two mirrors, realizing an optical oscillation. Since positive feedback can only be obtained for those modes that have an integer number of wavelengths in one round-trip of the cavity, each resonator will have a discrete set of resonant optical modes. Lasing occurs when amplification of photons in one of the optical modes is sufficient to overcome the existing losses.

Figure 1.13 features the different geometries that have been explored in the past years to obtain optical feedback. The first solid-state organic semiconductor laser was based on a vertical microcavity formed by a highly reflective dielectric mirror and a semi-transparent silver layer [132] (Fig. 1.13(a)). Following this study, there have been a number of reports about microcavity organic semiconductor lasers based on a broad range of materials [96, 171–173]. The fact that their fabrication is similar to the one of OLEDs and the fact that they emit perpendicular to the substrate, make this type of lasers particularly attractive. The distance traveled by the light during each pass through the gain medium, however, is rather small (mostly <100 nm), resulting in relatively high threshold values [174]. Only if high reflective dielectric mirrors are used at both sides of the microcavity, low laser thresholds can be obtained [172, 173, 175, 176].

Another way to achieve low laser thresholds is by using planar laser resonators where light is waveguided in the organic film via internal total reflection. In such a structure light is waveguided over much longer distances through the gain medium. The most simple way to fabricate a planar waveguide is by cleaving the organic film to obtain reflections at the facets. This is the most common approach used to fabricate low-cost inorganic semiconductor lasers, having very flat facets of typically 30% reflectivity. In contrast to inorganic semiconductors, however, breaking an organic film is rather difficult and does not result in high-reflective, high-quality facets. Nevertheless, lasing in such cavities has been successfully demonstrated [90, 96]. Superior performance can be achieved when feedback is incorporated via a

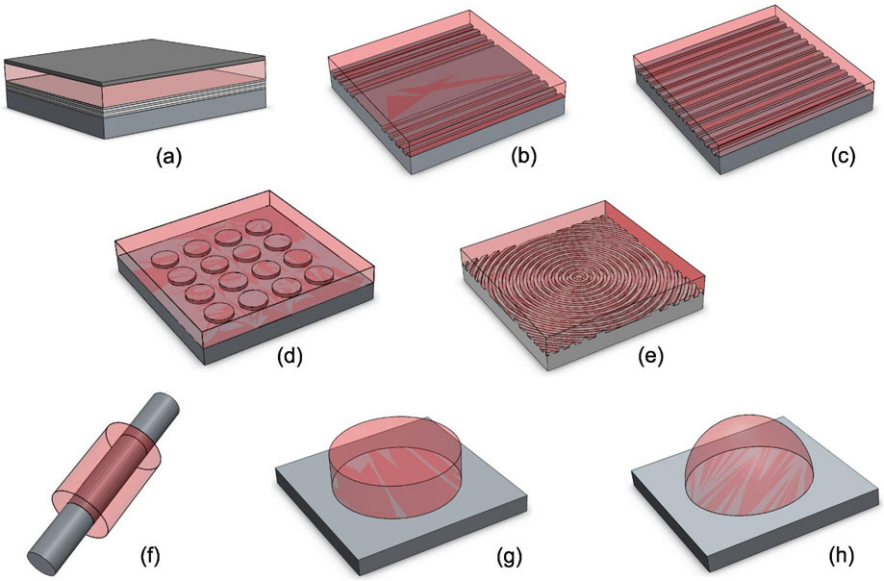

Fig. 1.13 Schematic representation of various resonator structures for optically pumped organic semiconductor lasers: (**a**) vertical microcavity, (**b**) distributed Bragg reflector (DBR), (**c**) distributed feedback (DFB) structure, (**d**) 2D photonic crystal structure, (**e**) circular DFB structure, (**f**) microring, (**g**) microdisk, and (**h**) microsphere

periodic perturbation of the waveguide giving rise to Bragg scattering. If Bragg gratings are placed outside the gain region, replacing the cleaved ends as wavelength selective mirrors, the structure is referred to as a distributed Bragg reflector (DBR) (Fig. 1.13(b)). Berggren *et al.* demonstrated such a laser comprising the small molecule blend Alq_3[8]:DCM_2[9] [114]. The Bragg grating can also be incorporated into the gain region. In this case one has reflection and transmission at every point in the cavity and thus the feedback is distributed throughout the entire length of the cavity. Lasers of this type are known as distributed feedback (DFB) laser, schematically shown in Fig. 1.13(c).

The concept of distributed feedback was introduced in 1971 by Kogelnik *et al.* [177, 178] and relies on Bragg scattering due to a periodic modulation of the refractive index or the gain of the active material. In distributed feedback structures lasing occurs near the Bragg wavelength λ_{Bragg}, which is given by the following relation:

$$\lambda_{Bragg} = \frac{2n_{eff}\Lambda}{m}, \quad m = 1, 2, \ldots. \tag{1.7}$$

Here, n_{eff} is the effective refractive index of the gain material, Λ is the modulation period of the DFB resonator and m is the DFB order number. For $m = 1$, first

[8]Tris-(8-hydroxyquinoline) aluminum.

[9]4-(dicyanomethylene)-2-methyl-6-(julolindin-4-yl-vinyl)-4H-pyran.

order diffraction is obtained, whereas for a second order DFB structure ($m = 2$) the wavelength of the reflected light equals $n_{eff}\Lambda$. In the latter case, laser radiation is also emitted perpendicular to the surface. This can be exploited for obtaining surface-emitting lasers. However, the out-coupled laser radiation represents a loss mechanism, explaining why higher laser thresholds are obtained for second- and higher-order DFB lasers compared to first-order DFB structures [146]. DFB lasers with one-dimensional feedback have been demonstrated using many different organic semiconductors, including derivatives of PPVs [179, 180], polyfluorenes [99, 141, 181] and LPPPs [182, 183], but also small molecule systems have been studied when deposited on top of DFB structures [184–186]. DFB lasers can exhibit very low laser thresholds. Threshold densities as low as 200 nJ/cm^2 have been reported for small molecule blends [184] and 40 nJ/cm^2 for conjugated polymers [148, 187]. DFB lasers also provide possibilities for the fabrication of tunable lasers. By changing either the period of the grating [98, 99, 102, 179, 188] or the thickness of the waveguide [103, 189], one may tune the lasing wavelength over a range of 20–50 nm. The largest tuning range was obtained using an Alq_3:DCM_2 blend, resulting in a tuning range of 115 nm [97].

Apart from one-dimensional DFB structures, also more complicated diffractive resonator structures have been reported. Two-dimensional (2D) feedback can, for example, be obtained in a 2D photonic crystal (Fig. 1.13(d)) with either square [147, 190–193], hexagonal [194] or honeycomb lattices [175]. Concentric circular DFB resonators (Fig. 1.13(e)) [195, 196] can also provide feedback in the plane of the organic semiconductor, although in this case feedback is applied in all directions from a single unique point that is located in the center of the grating. In contrast to their one-dimensional counterparts, 2D lasers exhibit improved output beam quality, lower threshold and higher output efficiencies [181, 190].

Other interesting resonator geometries to fabricate low threshold lasers are microring, microdisk and microsphere cavities (Fig. 1.13(f–h)). These lasers are typically larger in dimension than the vertical microcavities and hence the path traveled by the light through the gain medium in one round-trip is much longer. Consequently, much lower excitation densities are required to achieve sufficient gain [197, 198]. However, due to the long round-trip distance, these lasers have a rather complicated feedback mechanism that is based on a superposition of waveguide and whispering-gallery-mode oscillations [199–204].

Lowering the Lasing Threshold with Energy Transfer

One of the important criteria for active laser materials is the fact that the spectral overlap between stimulated emission and ground state absorption should be minimal in order to reduce self-absorption. Due to the presence of an inherent Stokes shift, the absorption spectrum and the emission spectrum of an organic material are shifted towards each other (Sect. 1.1.3). Most luminescent organic materials, however, still have a slight amount of residual absorption at the peak emission wavelength, reducing the overall gain that can be obtained. This self-absorption problem

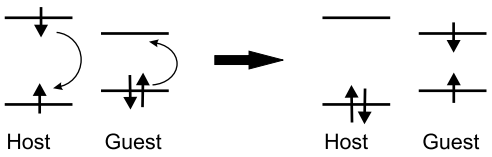

Fig. 1.14 Schematic description of Förster energy transfer

can be alleviated by shifting the emission to longer wavelengths, where residual absorption is smaller. Typically this is done by blending a small amount of a guest molecule or a polymer into a host matrix [90, 114, 135, 143, 205]. In such blends, the excited molecule non-radiatively transfers its energy to a neighboring molecule via long-range dipole-dipole coupling or electron exchange, also known as, respectively, Förster and Dexter energy transfer.

Förster energy transfer describes a radiationless transfer process that is caused by a coulombic interaction between a host and a guest molecule in close proximity (typically <10 nm). This process is shown in Fig. 1.14 and can be formally described by the interaction between the transition dipoles of the two molecules when the intermolecular distance is large enough (>1 nm) [21].

The rate of this energy transfer process k_{ET}^{F} is given by:

$$k_{ET}^{F} = \frac{9000\ln(10)\kappa^2\phi_{PL}}{128\pi^5 n^4 N_A \tau_H R^6}\int \lambda^4 f_H(\lambda)\varepsilon_G(\lambda)d\lambda, \tag{1.8}$$

where λ is the wavelength, $f_H(\lambda)$ is the normalized fluorescence spectrum of the host material, $\varepsilon_G(\lambda)$ is the absorption spectrum of the guest in terms of molar absorption coefficient, κ is a polarization factor, ϕ_{PL} is the absolute fluorescence efficiency of the host, τ_H is the radiative lifetime of the host, R is the mean distance between host and guest, N_A is the Avogadro constant and n is the refractive index of the medium. Equation 1.8 clearly indicates that for efficient energy transfer it is important to have a host with a high ϕ_{PL} and a guest with a high absorption coefficient. In addition, the overlap between $f_H(\lambda)$ and $\varepsilon_G(\lambda)$ has to be large. Since the energy transfer rate depends strongly on the distance between the molecules ($\sim R^{-6}$), the integral in Eq. 1.8 is often expressed in terms of the effective Förster radius, R_0:

$$R_0 = \left(\frac{9000\ln(10)\kappa^2\phi_{PL}}{128\pi^5 n^4 N_A}\int \lambda^4 f_H(\lambda)\varepsilon_G(\lambda)d\lambda\right)^{1/6} \tag{1.9}$$

which simplifies Eq. 1.8 to:

$$k_{ET}^{F} = \frac{R_0^6}{\tau_H R^6}. \tag{1.10}$$

Hence, the rate of Förster energy transfer between two molecules spaced at a distance $R = R_0$ equals the spontaneous emission rate of the host molecule $1/\tau_H$.

A good example of a Förster energy transfer system is the host-guest system Alq_3:DCM_2, for which an effective Förster radius R_0 of 39 Å has been calculated [96]. The strong overlap between the Alq_3 photoluminescence and the DCM_2 absorption spectra [114], results in efficient energy transfer from Alq_3 to DCM_2.

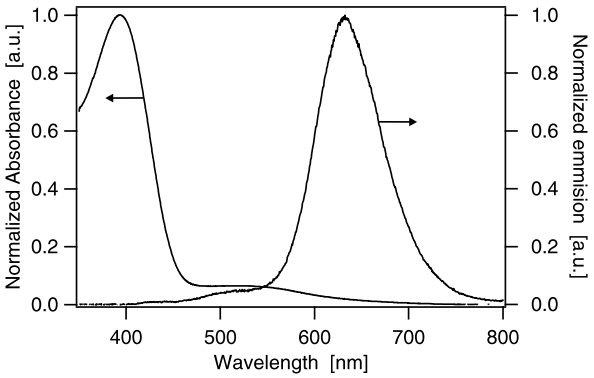

Fig. 1.15 Absorption and emission spectra of a composite Alq_3:DCM_2 thin film, comprising a 2%wt DCM_2 concentration. The absorption and emission spectral band are significantly shifted with respect to each other

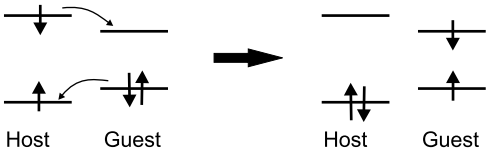

Fig. 1.16 Schematic description of Dexter energy transfer

This is demonstrated in Fig. 1.15. Although excitation was performed at a wavelength of 395 nm, which corresponds to the absorption maximum of Alq_3, the major emission originates from DCM_2, resulting in a very large Stokes shift (240 nm) between the absorption and emission spectral band of the Alq_3:DCM_2 film. Consequently, self-absorption is strongly reduced, making this material system very promising for laser applications. In literature there have been several reports on lasing action based on Förster energy transfer, demonstrating very low lasing thresholds [96, 114, 143, 184].

The Förster energy transfer process described above relies on strong coulombic interactions between the host and the guest. An alternative process for energy transfer, which is based on an electron exchange mechanism, may also be effective in the host-guest system. This process is referred to as Dexter energy transfer and is shown schematically in Fig. 1.16.

Similar to Förster energy transfer, the rate of Dexter energy transfer is proportional to the degree of overlap between the emission spectrum of the host and the absorption spectrum of the guest. However, the Dexter energy transfer rate is calculated using the normalized emission and absorption spectra, removing any dependence of the rate on the guest absorption coefficient. The rate of Dexter energy transfer k_{ET}^{D} is given by:

$$k_{ET}^{D} = \frac{2\pi}{h} \exp\left(\frac{-2R}{L}\right) K \int \lambda^4 f_H(\lambda) \varepsilon_G(\lambda) d\lambda, \tag{1.11}$$

where h is Planck's constant, L is the sum of the van der Waals radii of the host and the guest molecules and K is a constant proportional to the orbital overlap between host and guest. Since k_{ET}^{D} is proportional to $\exp(-2R)$, Dexter energy transfer is very fast for short distances between host and guest molecules (<1 nm), at larger

Table 1.1 Allowed energy transfer mechanism between an excited host molecule and a guest molecule in the ground state. The host molecule is the donor molecule D, whereas the guest molecule is the acceptor molecule A

Förster energy transfer	Dexter energy transfer
${}^1D^* + {}^1A \rightarrow {}^1D + {}^1A^*$	${}^1D^* + {}^1A \rightarrow {}^1D + {}^1A^*$
${}^3D^* + {}^1A \rightarrow {}^1D + {}^1A^*$	${}^3D^* + {}^1A \rightarrow {}^1D + {}^3A^*$

distances, however, its importance decreases rapidly. This is in contrast to Förster energy transfer, which is important at larger distances. Another important difference between Förster and Dexter energy transfer is related to the transitions that are allowed by both processes [21, 206]. While Förster energy transfer requires that the spin of the guest molecules stays unaltered, Dexter energy transfer, does not have a singlet requirement and can efficiently transfer energy between triplet states or between singlet states as long as the total spin symmetry is conserved. Therefore, Dexter energy transfer might still be important at larger distances for those transitions which are forbidden according to the Förster energy transfer process. An overview of mechanisms that are allowed to transfer energy from the excited host molecule to the singlet state of the guest molecule is given in Table 1.1. Both, Förster and Dexter energy transfer can be the mechanism for singlet-singlet energy transfer. However, Förster energy transfer will be the dominant mechanism at low guest concentrations because it is faster over long distances.

1.3.4 Prospects for Electrically Pumped Organic Lasers

Looking at the impressive way in which organic semiconductor materials have become established as new laser materials during the last decade, it is not surprising that main efforts now focus on the development of electrically pumped organic lasers [91]. Electrical pumping is the most convenient way to achieve lasing and is the approach used in inorganic semiconductor diode lasers.

It is expected that high current densities are required to achieve sufficient gain for stimulated emission in organic semiconductors. From optically pumped laser experiments, a lower limit of the current density required to reach lasing threshold can be estimated. Kozlov *et al.* calculated that a current density threshold of 80 A/cm^2 would be needed to obtain stimulated emission in a DFB laser with a DCM[10]-doped Alq_3 emissive layer sandwiched between two cladding layers of Alq_3 [184]. A similar estimation has been made for polymer DFB structures [85]. Several research groups demonstrated that this level of injection can be achieved in organic semiconductors under pulsed operation [207–209]. Recently, current densities as high as 12000 A/cm^2 [210] and 128000 A/cm^2 [211] have been reported in thin films

[10] 4-(dicyanomethylene)-2-methyl-6-[(4-dimethylaninostyryl)-4H-pyran.

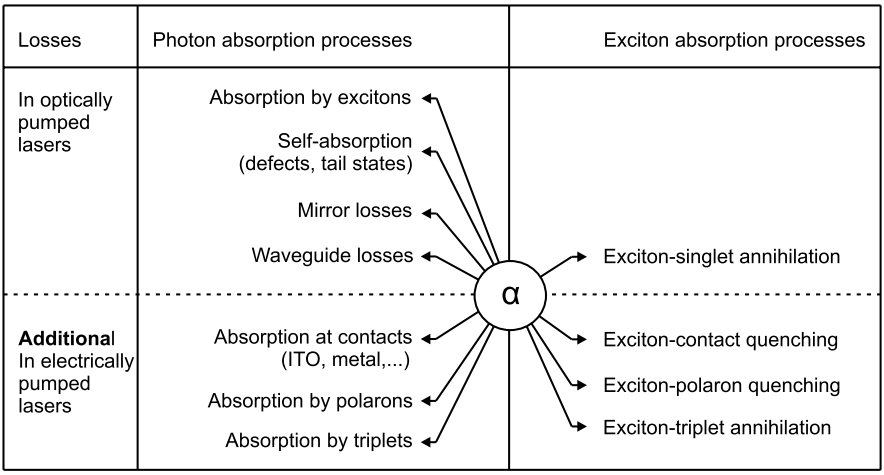

Fig. 1.17 Overview of the possible losses encountered in optically pumped lasers and the additional losses that can be expected in electrically pumped lasers

of copper phthalocyanine. Although this material is not suitable for lasing, it shows that organic semiconductors can sustain extremely high current densities, exceeding the estimated current density threshold by several orders of magnitude. On the other hand, it also demonstrates that the difficulties to realize electrically pumped organic lasers today must be attributed to the presence of additional loss mechanisms compared to optically pumped lasers. Figure 1.17 gives an overview of these additional losses. The figure summarizes the possible losses encountered in optically pumped lasers as well as the additional losses that can be expected in electrically pumped laser devices. A distinction is made between losses of excitons (right column), that make it more difficult to achieve a high N_{exc} in the gain formula (Eq. 1.5), and losses of photons, that result in a higher gain coefficient to be required to achieve stimulated emission: indeed, $g_{min} = \sum \alpha_{photon}$.

Only fluorescent systems, based on singlet emission, can efficiently be pumped by optical excitation. Consequently, the 'exciton-singlet' annihilation process in the right column of Fig. 1.17 refers to singlet-singlet annihilation. At typical threshold concentrations of singlets for lasing, $N_{exc} \sim 10^{17} - 10^{18}$ cm^{-3} [154, 184], this mechanism is not dominant in amorphous organic thin films [85, 212]. Absorption of photons by excitons and self-absorption can be minimized by the choice of material [85]. An appropriate choice of the resonator structure may then further reduce the optical losses. As mentioned in Sect. 1.3.3 mirror losses can be minimized by using diffractive resonator structures. As a result of such optimizations, low losses are possible and optically pumped organic lasers having low laser thresholds can be obtained [146, 184, 187]. On the other hand, to obtain lasing by electrical pumping several other loss mechanisms should still be suppressed.

A first challenge to achieve electrically pumped lasing is to overcome the additional losses due to absorption of photons at the electrical contacts. This is particularly important for organic semiconductor lasers where the resonator is positioned

in the plane of the film. In these lasers a long interaction length is present between the light and the gain medium. However, this also means that there is a long interaction with the electrical contacts, which absorb light. Therefore, optical losses in thin waveguide structures including electrodes are very substantial [96]. This was demonstrated by Andrew *et al.*, who reported a considerable increase of the lasing threshold of a MEH-PPV-based organic DFB laser upon inserting a thin silver layer [213]. These detrimental waveguide losses, however, may be reduced by careful optical design [182, 214]. In literature different device architectures have been proposed to reduce the losses caused my metallic layers. A possible strategy is to increase the total thickness of the organic layer stack, by separating the emissive layer from the electrodes by cladding layers that transport the injected electrons and holes towards the active light-emitting layer [84, 215]. In this way the absorption losses at the electrical contacts can be reduced. However, because of the typical low carrier mobility of organic semiconductors [31, 32], the thickness of the organic layers cannot be arbitrary increased. In order to ensure efficient charge transport the total thickness of organic layers is generally limited to less than 200 nm [96]. To circumvent this problem, the use of transparent conductive oxides (TCO) such as indium tin oxide (ITO) [44] and aluminum doped zinc oxide (AZO) [216] has been proposed. A reduction of the organic stack thickness is possible if thin layers of these materials are used as electrical contacts in waveguide structures [96, 217, 218]. This is mainly due to the much lower optical losses in the visible spectral range of TCO layers compared to metallic layers [184]. Görrn *et al.* demonstrated that positioning TCO contacts in the intensity minima of the TE_2 waveguide mode, allows even further minimization of the overlap between the optical mode and the contacts [219]. In addition, Reufer *et al.* reported that it is also possible to use thick, more conductive ITO layers, provided that a cross-linked hole-transport layer is inserted between the highly conductive ITO and the emission layer [220]. Besides conventional LED devices, organic light-emitting transistors (LEOFETs, Sect. 1.2.2) have been suggested as potential laser structures [49, 65, 69, 75, 221, 222]. This configuration makes it possible to position the light-emission zone far away from the metal electrodes and allows minimization of the charge carrier density because of the high field-effect mobility of the carriers. In addition, very high current densities, exceeding several kA/cm^2, have been demonstrated in these devices [63, 69, 75].

Another source of losses associated with electrical pumping is related to the presence of polarons. Electrical excitation involves charge injection. As discussed in Sect. 1.1.1, the injected charges together with their polarization are referred to as polarons. These polarons may cause additional absorption losses [184, 209, 223, 224] and may deplete the exciton population via exciton-polaron quenching [212, 215]. Polaron absorption can be measured by using electro-optical pump and probe experiments and has been observed in polymer [209] as well as in small molecule [184, 207] light-emitting devices. Typically, the polaron absorption spectrum is very broad and covers a wide spectral range. For PPV, for example, the polaron absorption spectrum extends from the ground state absorption band edge to the IR and overlaps with the gain spectrum of the material [225]. Since for low mobility organic semiconductor materials, such as PPV, there are under steady-state conditions much

more polarons than singlets [84, 209], polaron absorption will be stronger than stimulated emission, creating a problem for lasing. Several approaches are suggested in literature to avoid the problems related to polaron absorption and polaron quenching [85, 225]. The most obvious solution is to develop a material system where the polaron absorption is shifted with respect to the spectral region of stimulated emission [84, 184]. However, this might not be trivial to find due to the broad nature of polaron absorption. Another possibility is to use organic semiconducting materials with high charge carrier mobility [84, 223]. This would reduce the required charge density in the device, making polaron-exciton quenching and polaron absorption less problematic. A third approach is to operate the device under pulsed excitation [225, 226]. Pulsed operation has several advantages: it avoids heat and stress in the device [227], it allows higher current densities compared to continuous-wave (CW) operation [209], and it makes it possible to separate singlet excitons from polarons in the time domain. This time separation would allow a tremendous reduction of polaron absorption in an electrically driven organic light-emitting device [228].

Besides polarons, current injection also leads to the formation of triplet excitons. As can be seen from Fig. 1.17 these triplet excitations form a third major obstacle to obtain electrically pumped lasing. The inevitable population and accumulation of triplets under electrical excitation results in excessive triplet-state losses preventing lasing [50, 223, 229]. Indeed, if conventional spin statistics apply, the recombination of injected charge carriers leads to the creation of a majority (75%) of non-emissive triplet excitations in the active organic semiconductor layer [36]. Due to their long lifetime, these triplet excitations can act as meta-stable species, which generally have fairly high absorptions to the upper triplet state (triplet-triplet absorption) at the expected fluorescent lasing wavelength [223, 228]. In addition, at high brightness conditions triplets may also severely quench singlet excitons, reducing N_{exc} [50, 212, 215]. Similar to the approach for reducing the amount of polarons in the device, pulsed operation can also be used to separate singlets from triplets in the time domain [228]. By applying pulses which have a pulse duration longer than the singlet lifetime (typically 1 ns) and shorter than the lifetime of triplet excitons (milliseconds to seconds for fluorescent materials) [230], and assuming the pulse repetition rate is low, the accumulation of triplet excitons can be reduced. In this way triplet state losses such as singlet-triplet annihilation and triplet-triplet absorption might be suppressed. The use of appropriate triplet scavengers is also proposed as an alternative way to reduce triplet accumulation [50].

In fact, the critical issues outlined above are mainly related to the low charge carrier mobility of organic semiconductors. The low mobility makes it difficult to obtain high current densities, it prevents the use of thick organic layers to reduce absorption at the metallic contacts and it increases the number of charge carriers needed to generate population inversion in the device. Hence, the use of new materials with higher mobilities would help with each of these issues. Combining a high mobility with simple processing and high photoluminescence efficiency is, however, a challenging project. Therefore, an intermediate solution based on indirect electrical pumping has been proposed, allowing compact and low-cost tunable laser devices [229, 231]. In these devices solid-state inorganic laser diodes are used to

pump an organic laser structure optically, circumventing problems associated with electrical pumping. Several demonstrations of indirect electrically pumped lasing in hybrid laser devices have been reported [99, 231, 232].

Recently, spectrally narrowed emission from electrically pumped organic semiconductor films has been demonstrated. Yokoyama *et al.* observed spectrally narrowed emissions from the edges of electrically pumped OLEDs comprising BSB-Cz[11] [233]. These emission spectra corresponded well to the cutoff wavelength of the waveguide structure. In addition, the edge emission intensity of the TE mode showed a superlinear dependence on the current density. The combination of both effects has been attributed to the occurrence of light amplification. Tian *et al.*, however, reported that the apparent "optical gain" associated with spectrally narrowed edge emission from OLEDs, might also result from misalignment of the propagating leaky waveguide modes and the collecting optics [234]. Very recently, Liu *et al.* reported lasing action in an electrically pumped microcavity device [176]. The device showed a threshold current density of 860 mA/cm^2 under room temperature pulsed operation. However, if the observed emission is real laser emission is still under debate. The rather strange spectral behavior of the device as function of the current, the limited spectral narrowing and the fact that spacial coherence can also be the result of other factors, such as a small pumping area or a decrease in the current spreading, might suggest that the observed emission origins from a microcavity-OLED rather than from a laser device.

1.4 Outline

In this first chapter, the basic principles of organic optoelectronics were highlighted and the state-of-the-art light-emitting devices as well as the challenges that have to be overcome to achieve electrically pumped lasing were discussed. The following chapters of this book focus on the design of new device and material concepts for organic light-emitting devices. Main attention is thereby given to the control of the triplet density and to the possibility to achieve high current densities combined with reasonable efficiencies and reduced absorption at metallic contacts. In this respect the proposed concepts offer new prospects for the realization of solid-state high-brightness organic light sources.

Chapter 2 starts with an overview of the organic materials and the experimental techniques that were used during this work. Sample fabrication as well as the different methods used to characterize the devices are discussed.

In Chap. 3, an OLED with field-effect electron transport is proposed as a new device architecture complementary to the list of existing electroluminescent devices. The device is a hybrid structure between a diode and a field-effect transistor. It allows minimization of the optical absorption losses and the charge carrier density in the device, while at the same time high current densities can be achieved. Device

[11] 4,4'-bis[(N-carbazole)styryl]biphenyl.

fabrication and operation are discussed in detail. The electrical characteristics and the opto-electronic performance of the device are measured and are compared with numerical simulations.

Improving the device performance is the subject of Chap. 4. Two diperfluorohexyl-quater thiophene derivatives are investigated for use as the electron-trans porting material in OLEDs with field-effect electron transport. First, the growth conditions of both materials are optimized and high-mobility field-effect transistors are fabricated. Using the optimized growth conditions OLEDs with field-effect-assisted electron transport are fabricated and their electrical characteristics are measured. A comparison between the performance of different devices comprising various electron-transporting materials is given at the end of this chapter.

Chapter 5 presents methods to control the triplet concentration in electrically driven devices. A first method to control triplet accumulation is by operating the device under pulsed excitation. The behavior of OLEDs with field-effect-assisted electron transport is analyzed under these conditions and their performance is compared to conventional OLEDs comprising the same set of materials. Experiments to identify the limiting factors with respect to the pulse width dependence of the light-emitting devices are performed. An alternative way to reduce the triplet population is investigated in the second part of this chapter. Polymer films doped with a nonvertical triplet scavenger are studied by time-resolved photoluminescence measurements. The results are compared to those obtained by using a vertical triplet acceptor, which also possesses suitable energetic levels to scavenge host triplets.

Triplet dynamics and charge carrier trapping in triplet-emitter doped conjugated polymers are the focus of Chap. 6. Phosphorescent properties and charge carrier trapping are studied by means of time-resolved photoluminescence and thermally-stimulated luminescence techniques. In this chapter also the route of using triplet-emitters as light-emitting species in the active layer of an organic laser is investigated. Three different phosphorescent compounds are carefully checked, however, no stimulated emission could be observed.

In Chap. 7, the value of OLEDs with field-effect-assisted electron transport as laser device configuration is discussed. The reduced absorption losses compared to conventional OLED structures are analyzed. Amplified spontaneous emission measurements and optically pumped lasing experiments are performed on organic layer stacks including hole- and electron transporting layers used in OLEDs with field-effect-assisted electron transport. In addition, the different possibilities to incorporate an optical feedback mechanism in the device are discussed.

Finally, conclusions are drawn and some outlook for future research is given in Chap. 8.